Formation of Chromia from Amorphous Chromium Hydroxide

Svetozar Musić,[a,*] *Miroslava Maljković,*[a] *Stanko Popović,*[b] *and Rudolf Trojko* [a]

[a] *Ruđer Bošković Institute, P. O. Box 1016, HR–10001 Zagreb, Croatia*

[b] *Department of Physics, Faculty of Science, University of Zagreb, P. O. Box 162, HR–10001 Zagreb, Croatia*

Forced hydrolysis of $Cr(NO_3)_3$ in a solution of decomposing urea was investigated. Chromium hydroxide precipitates were amorphous for the final pH values up to ~9 to 9.5. Heating of amorphous chromium hydroxide up to 360 °C produced Cr_2O_3 crystallites of the order of 20 nm, whereas after heating up to 825 °C the crystallite size of Cr_2O_3 increased to the order of 100 nm. Crystallization of Cr_2O_3 was also monitored by FT-IR spectroscopy. TGA/DTA curves, recorded in air, showed thermal behavior of amorphous chromium hydroxides that differed depending on the experimental conditions of their preparation. A sharp exothermic peak between 410 and 420 °C was recorded due to the crystallization of Cr_2O_3. This peak shifted to 600 °C when the heating of amorphous chromium hydroxide was performed in an argon atmosphere. Accelerated crystallization of Cr_2O_3 from amorphous chromium hydroxide in air is explained by the catalytic effect of the higher oxidation states of chromium species, which were probably restricted to the surface of the particles. It is suggested that higher oxidation states of chromium were not stable and they converted to the initial Cr(III) state. XRD did not detect any oxide phase of chromium except for Cr_2O_3.

Key words: chromia, amorphous chromium hydroxide, crystallization, FT-IR spectroscopy, X-ray powder diffraction

* Author to whom correspondence should be addressed.

INTRODUCTION

Chromium oxides (Cr_2O_3, CrO_2, CrO_3) and oxyhydroxide (CrOOH) have been extensively investigated from different standpoints. Possible industrial applications of these compounds depend on their chemical, physical and microstructure properties. Generally, the properties of these compounds can be modified by synthesis conditions. For this reason, in many investigations, researchers have tried to establish the relation between the properties of chromium oxides and synthesis conditions. Special attention was focussed on the formation and properties of chromia (Cr_2O_3), which have found important application in high-temperature resistant materials, solar energy collectors, liquid crystal displays, catalysts, *etc*. Cr_2O_3 was also detected in the rust formed by corrosion of Cr-containing steels. In this introduction, we shall focus attention on selected works in the literature dealing with chromium hydroxide ($Cr(OH)_3$) and Cr_2O_3.

Colloidal $Cr(OH)_3$ particles of narrow size distribution were prepared by heating diluted $KCr(SO_4)_2$ solution.[1] The basic chromium sulfate polymer served as precursor or heteronucleating agent in the precipitation of the $Cr(OH)_3$ colloids. The possible chemical reactions involved in the precipitation of the $Cr(OH)_3$ colloids were discussed.[2,3] Surface properties of the $Cr(OH)_3$ were investigated[4] in dependence on the time of heating of $KCr(SO_4)_2$ solution ($4 \cdot 10^{-4}$ mol dm^{-3}) at elevated temperature. Sulfate ions had a chief role in the process of Cr^{3+} hydrolysis. The surface properties of amorphous Cr_2O_3 particles and the thermal decomposition products of the starting material were also investigated[5] using acid-base potentiometric titrations. Specific adsorption of sulfates on the particles was observed. Specifically adsorbed sulfates could be desorbed by alkaline washing, but not by acidic washing. Siddiq *et al.*[6] observed that the surface area of chromium hydroxide gels strongly decreased with an increase of the precipitation pH from ~5 to ~11. This effect was explained by the nature of the chromium hydroxide gel, which is more polymeric at low pH and crystalline at pH > 10.

Chromium hydroxide gel was precipitated from $Cr(NO_3)_3$ solution adding hydrazine monohydrate.[7] Crystallization of Cr_2O_3 was observed at 380 to 405 °C. The lattice parameters of Cr_2O_3 (in terms of hexagonal axes), prepared by heating the gel at 450 °C for 1 h, were $a = 0.4955$ nm and $c = 1.359$ nm, the space group being $R\bar{3}c$. Cr_2O_3 pellets having 98.9% of theoretical density were produced by hot isostatic pressing at 1100 °C for 2 h and 196 MPa. Hou *et al.*[8] dissolved $Cr(NO_3)_3 \cdot 9H_2O$ in water and, after heating the solution to dryness, the solid residue was sintered and heated up to 1000 °C. Less than 1% CrO_2 was estimated in all samples. The samples obtained after heating at 400 to 600 °C showed phases with crystallite size of 17 to 25 nm, respectively. Thin Cr_2O_3 films were prepared by the CVD method using chromium acetylacetonate and chromium hexacarbonyl.[9] In the case of

chromium hexacarbonyl, the reaction temperature could be decreased from 150 to 60 °C by irradiation with UV light.

Maciejewski *et al.*[10] investigated the thermal decomposition of the $Cr(NO_3)_3 \cdot 9H_2O$ salt and observed the formation of CrO_2 as a stable phase. The ratio of CrO_2 to Cr_2O_3 depended on the heating conditions of the starting salt. For complete phase transformation to Cr_2O_3, a temperature higher than 600 °C was required. Rapid crystallization of the amorphous intermediary, obtained at lower temperatures, produced Cr_2O_3 as a single phase at ~380 °C. The phase transformation $CrO_2 \rightarrow CrOOH$ (yield ~95%) and the reversibility of this phase transformation were observed under specific experimental conditions.

In a research into chromium oxides, significant attention was paid to the characterization of chromium oxides supported on various oxide carriers. SiO_2 and γ-Al_2O_3 were impregnated[11] with the $Cr(NO_3)_3 \cdot 9H_2O$ salt, $Cr_2O_3 \cdot 5H_2O$ gel or CrO_3 and then the oxides were heated at 600 °C for 5 h. The Cr_2O_3 particles on SiO_2 were predominant, while dispersed chromates were observed on γ-Al_2O_3, irrespective of the type of the precursor used. Differences in the composition of coatings were explained by differences in the surface chemistry and population of terminal OH groups on the adsorbents. Vuurman *et al.*[12] also found differences in the chromium oxide coatings on SiO_2 adsorbent, on one the hand, and on Al_2O_3, TiO_2 and ZrO_2 adsorbents, on the other. Diffuse reflectance spectroscopy[13] and Raman spectroscopy[14] were used to investigate the oxidation state of chromium and the nature of the chromium-oxygen bond. TiO_2 particles were impregnated[15] with $Cr(NO_3)_3 \cdot 9H_2O$ and then heated under different conditions. X-ray absorption near edge structure (XANES) of the samples indicated Cr_2O_3 and CrO_2 in the coatings, whereas the presence of chromates and/or CrOOH was not confirmed. Baiker *et al.*[16–20] systematically investigated chromium oxide coatings on TiO_2 adsorbent. This catalyst is important in the selective catalytic reduction (SCR) of nitric oxide (NO) with ammonia in the presence of an excess of oxygen. Amorphous chromia was found to be more active and selective to N_2 formation than crystalline chromia. Musić *et al.*[21,22] investigated the Cr_2O_3–Fe_2O_3 system using XRD and spectroscopic techniques. Rousset and Pâris[23] also investigated the formation of solid solutions in the Cr_2O_3–Fe_2O_3 system.

In the present work, we focus on the forced hydrolysis of a solution of $Cr(NO_3)_3$ and urea. Selected samples of amorphous chromium hydroxides, obtained as hydrolytic products, were subjected to thermal treatment in order to ascertain the conditions of the phase conversion of amorphous $Cr(OH)_3$ to the oxide phase. The results of the present investigation are important for engineers involved in the production of thin chromium oxide films or catalysts.

EXPERIMENTAL

The $Cr(NO_3)_3 \cdot 9H_2O$ salt and urea of analytical purity were used. The solutions were prepared using doubly distilled water. Hydrolysis experiments were performed using an oil bath (± 1 °C) with reflux. For long period of times (1 day and more) the precipitation systems were aged under autoclaving conditions. After an appropriate aging time, the suspensions were centrifuged to separate the precipitate from mother liquor. An ultra-speed centrifuge, Sorvall RC2-B, with an operational range up to 20000 r.p.m. was used. Precipitates were subsequently washed with doubly distilled water and dried. The history of selected samples is given in Table I. Commercial Cr_2O_3 (purity 99.999%) supplied by Ventron was also used.

The pH of the mother liquor was measured using a pH-meter, model pHM–26, manufactured by Radiometer. A combined glass/calomel electrode with an operational range up to pH 14, also manufactured by Radiometer, was used.

X-ray powder diffraction (XRD) patterns were taken using an automatic Philips diffractometer, model MPD 1880 (Cu$K\alpha$ radiation, graphite monochromator, proportional counter). From the broadening of the diffraction lines of Cr_2O_3, the crystallite sizes were estimated using the Scherrer equation

$$D = 0.9\,\lambda\ /\ (\beta \cdot \cos\theta)$$

where λ is the X-ray wavelength, θ is the Bragg angle and β is the pure full width of the diffraction line at half the maximum intensity.

TABLE I

History of the samples

Sample	Experimental conditions
C1	Hydrolysis of the solution 0.1 M $Cr(NO_3)_3$ and 0.5 M urea at 100 °C for 9 h. pH_{final} = 7.05
C2	Sample C1 was heated in air up to 240 °C at the rate 10 °C/min
C3	Sample C1 was heated in air up to 290 °C at the rate 10 °C/min
C4	Sample C1 was heated in air up to 360 °C at the rate 10 °C/min
C5	Sample C1 was heated in air up to 825 °C at the rate 10 °C/min
C6	Hydrolysis of the solution 0.1 M $Cr(NO_3)_3$ and 1.0 M urea at 100 °C for 9 h. pH_{final} = 8.07
C7	Sample C6 was heated in air up to 825 °C at the rate 10 °C/min
C8	Hydrolysis of the solution 0.1 M $Cr(NO_3)_3$ and 2.0 M urea at 100 °C for 9 h. pH_{final} = 8.92
C9	Sample C8 was heated in air up to 825 °C at the rate 10 °C/min.
C10	Hydrolysis of the solution 0.1 M $Cr(NO_3)_3$ and 0.3 M urea at 90 °C for 3 days. pH_{final} = 8.37
C11	Sample C10 was heated in argon up to 650 °C at the rate 10 °C/min and then cooled also in argon

The FT-IR spectra were recorded using a Perkin-Elmer spectrometer (model 2000). The spectra were processed using the Infrared Data Manager (IRDM) program also supplied by Perkin-Elmer. The specimens were pressed into KBr matrix.

Thermal analysis was performed using an instrument produced by Netzsch. The temperature was controlled by a Pt-PtRh(10%) thermocouple, and the heating rate was 10 °C min^{-1}. TGA/DTA instrumentation was also used for the heating of amorphous chromuim hydroxide under controlled conditions to obtain thermal decomposition products for further instrumental characterization.

RESULTS AND DISCUSSION

In aqueous medium, urea undergoes hydrolysis at elevated temperatures in accord with the chemical reaction:

$$(NH_2)_2CO + 3\ H_2O\ \rightarrow\ 2\ NH_4^+ + 2\ OH^-\ + CO_2$$

Increase of the pH-value in a solution of decomposing urea depends on the initial concentration of urea, temperature and time of heating. Figure 1 illustrates the dependence of pH on time during the forced hydrolysis of $Cr(NO_3)_3$ solution in decomposing urea in autoclaving conditions. In the presence of decomposing urea, a significant pH-increase under control conditions can be achieved, and in the present work this effect was used to accelerate the hydrolysis of Cr^{3+} ions for the precipitation of the hydroxide phase. The analysis of the precipitates showed their amorphous character, even for the precipitates obtained at relatively high pH values (pH ~9 to 9.5) and for long times of aging, up to 60 days.
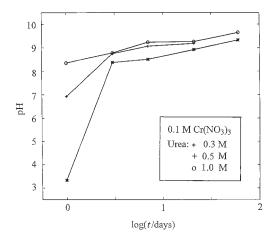

Figure 1. Dependence of pH on the time of the forced hydrolysis at 90 °C of 0.1 M $Cr(NO_3)_3$ solution with varying initial concentrations of urea.
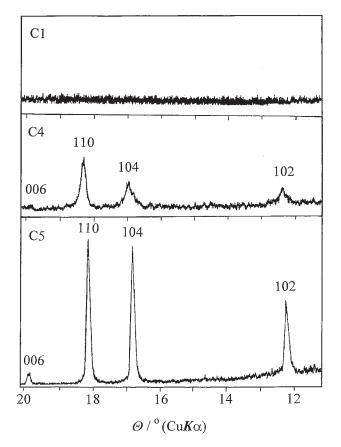
Figure 2. Characteristic parts of X-ray powder diffraction patterns of amorphous chromium hydroxide (sample C1) and its thermal decomposition products (samples C4 and C5). Diffraction patterns were recorded at room temperature.

Figure 2 shows characteristic parts of the X-ray powder diffraction patterns of sample C1 and its thermal decomposition products. It can be seen that sample C1 is completely amorphous. After the heating of sample C1 up to 290 °C, the thermal decomposing product was amorphous, as proved by XRD. With an increase of the heating temperature up to 360 °C, crystalline Cr_2O_3 appeared as well as an amorphous fraction (sample C4). On the basis of the broadening of diffraction lines, it was estimated that the crystallite size of Cr_2O_3 (sample C4) was of the order of 20 nm. In nanotechnology, it is generally assumed that particles up to ~30 nm belong to the so-called nano-sized range. We note that particle size differs from crystallite size by definition; however, in the case of very small particles their size is often comparable with the crystallite size, as estimated by the Scherrer formula. After
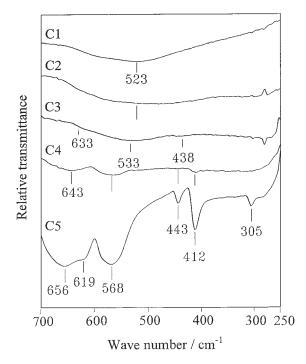
Figure 3. FT-IR spectra of amorphous chromium hydroxide (sample C1) and its thermal decomposition products (samples C2, C3, C4 and C5). The spectra were recorded at room temperature.

heating sample C1 up to 825 °C (sample C5), crystalline Cr_2O_3 was detected with slightly broadened X-ray powder diffraction lines. The crystallite size of Cr_2O_3 in sample C5 and those estimated for the samples obtained by heating other chromium hydroxide precipitates up to 825 °C were of the order of 100 nm. Also, the crystallite shape of samples C4 and C5 was a little asymmetric, thus showing a smaller dimension along the c-axis.

Figure 3 shows the FT-IR spectra of sample C1 and its thermal decomposition products (samples C2 to C5). Sample C1 was characterized by a very broad band centered at 523 cm^{-1}. A similar spectrum was also recorded for sample C2. In the spectrum of sample C3, a very broad IR band was centered at 533 cm^{-1}. A weak shoulder at 633 cm^{-1} and a weak band at 438 cm^{-1} are visible, indicating a certain level of structural ordering in the amorphous phase. The IR bands characteristic of Cr_2O_3 were visible in the spectrum of sample C4 and they were well developed in the spectrum of sample C5. Figure 4 shows FI-IR spectra of samples C7 and C9 with the bands typical of Cr_2O_3, and the spectrum of commercial Cr_2O_3 (purity 99.999%). The FT-IR spectra of samples C5, C7, C9 and commercial Cr_2O_3
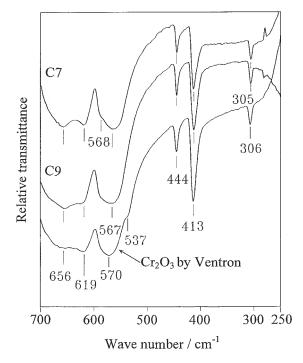
Figure 4. FT-IR spectra of Cr_2O_3 (samples C7 and C9) and commercial Cr_2O_3 by Ventron (purity 99.999%). The spectra were recorded at room temperature.

show relative differences in the intensities of the shoulders at 656 and 619 cm^{-1}. Commercial Cr_2O_3 also showed a shoulder at 537 cm^{-1}. These differences can be related to the differences in crystallinity, particle size and shape of the Cr_2O_3 samples.

The IR spectrum of Cr_2O_3 was investigated by several researchers and, here, only selected works will be reviewed. Renneke and Lynch[24] investigated the IR modes of Cr_2O_3 using a classical oscillator analysis of its reflectivity data. The modes vibrating parallel to the *c*-axis occurred at 538 and 613 cm^{-1}, whereas the modes vibrating perpendicular to the *c*-axis occurred at 417, 444, 532 and 613 cm^{-1}. Serna *et al.*[25] recorded IR spectra for Cr_2O_3 having dominantly lath-type particles. Small contributions of cylinder- or sphere-type particles were related to the broad shoulder at 650 to 700 cm^{-1}. For the dominant morphology, the bands at 617, 556, 443 and 305 cm^{-1} were ascribed to E_u modes, whereas the bands at 415 and approximately 720 cm^{-1} were ascribed to A_{2u} modes. The characteristic IR bands were used to identify the Cr_2O_3 phase in the rust formed by the high-temperature corrosion of the alloy Inconel 718.[26] IR spectroscopy was also applied in the investigations[27–29] of Cr_2O_3 surface chemistry.
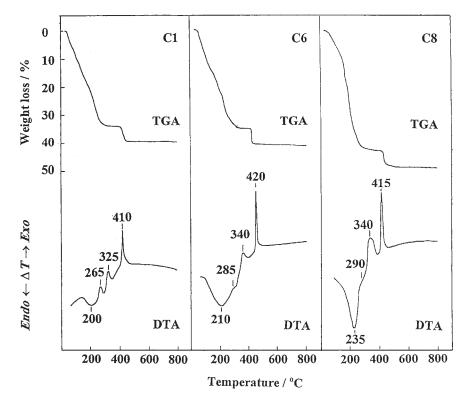
Figure 5. TGA/DTA curve of amorphous chromium hydroxide (samples C1, C6 and C8) obtained in air.

Figure 5 shows TGA/DTA curves of amorphous chromium hydroxide (samples C1, C6 and C8). In spite of the fact that all these samples were amorphous, the DTA curves indicated that their thermal behavior differed depending on the hydrolysis conditions, *i.e.* the initial concentration of urea. Sample C1 showed a broad endothermic peak centered at 200 °C and intersected by two exothermic peaks at 265 and 325 °C. A sharp exothermic peak corresponding to Cr_2O_3 crystallization was positioned at 410 °C. XRD analysis showed that Cr_2O_3 crystallization started at lower temperatures (Figure 2, sample C4). The DTA curve of sample C6 showed a shoulder at 285 °C, whereas the DTA curve of sample C8 showed a shoulder at 290 °C. The second exothermic peak shifted from 325 to 340 °C in the order C1→C6→C8.

Carruthers *et al.*[30] heated chromium oxide gel in an oxygen atmosphere and observed exothermic peaks at 230 and 280 °C and a sharp exothermic peak at 400 °C. Heating in nitrogen atmosphere shifted the Cr_2O_3 crystallization peak from 400 to 580 °C. It was concluded that the crystallization of

Cr_2O_3 at lower temperatures in an oxygen atmosphere was promoted by a fast oxidation reaction Cr(III)→Cr(VI). Measurements of the surface area (B.E.T.) of the thermal decomposition products of chromium oxide gel in air, vacuum or dry nitrogen[31] showed a shift of maximum surface area to ~400 °C in the case of nitrogen atmosphere. It was also concluded that the exothermic peak at ~230 °C is due to the formation of orthorhombic CrOOH. Ratnasamy and Léonard[32] neutralized 0.1 M $Cr(NO_3)_3$ solution with NH_4OH solution up to pH 10.5. The authors reported that the precipitated chromium hydroxide possessed a crystalline structure. Water molecules were eliminated from the hydroxide precursor below 200 °C and crystalline Cr_2O_3 was produced at 400 °C. It was also concluded that samples produced up to 240 °C have a »short-range structure« similar to that in $HCrO_2$. Klissurski and Bluskov[33] neutralized $Cr(NO_3)_3$ solution with NH_4OH solution at pH 7 to 8. The authors suggested surface formation of $HCrO_2$ during the heating of chromium hydroxide at lower temperatures. The exothermic peak, due to Cr_2O_3 crystallization was observed at 380 °C for humid air and at 400 °C for dry air. Giovanoli and Stadelmann[34] detected only Cr_2O_3 during thermal decomposition of crystalline $Cr(OH)_3 \cdot 3H_2O$. By decomposition of crystalline $Cr(OH)_3 \cdot 3H_2O$ under water vapor, a short range order developed up to 300 °C, which may be attributed to very fine crystallites of CrOOH.

In order to investigate the influence of the atmosphere on the heating of amorphous chromium hydroxide, as prepared in the present work, we performed the experiment in an argon atmosphere. The sample was cooled to room temperature, also in an argon atmosphere, to avoid the possible sample oxidation during the cooling. Figure 6 shows the DTA curve of sample C10 obtained in an argon atmosphere. A strong endothermic peak at 200 °C, due to water loss, was visible. The sharp and very strong exothermic peak shifted to 600 °C. Figure 7 shows FT-IR spectra of amorphous chromium hydroxide (sample C10) and the thermal decomposition product obtained at 650 °C in an argon atmosphere (sample C11). Sample C10 showed a typical FT-IR spectrum of amorphous chromium hydroxide with a very broad band centered at 523 cm^{-1}. However, the FT-IR spectrum of sample C11 showed a certain difference in relation to the spectra of Cr_2O_3 obtained by heating amorphous chromium hydroxide in air. The IR band at 619 cm^{-1} was pronounced and the band at 656 cm^{-1}, shown in Figure 4, was strongly suppressed. Also, the relative intensity of the IR band at 412 cm^{-1} was strongly decreased. Precise X-ray powder diffraction (bulk analysis) of sample C11 did not indicate the presence of nonstoichometric $Cr_2O_{3-\delta}$ (δ = loss of oxygen) or other oxide phases besides Cr_2O_3. Another factor that might have influenced the shape of the FT-IR spectrum was the particle size and shape or the sintering effect.[25] Also, the exothermic shift to 600 °C in the DTA curve,
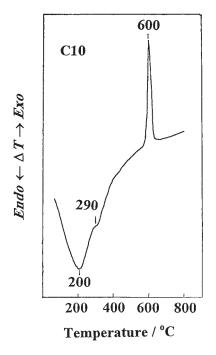
Figure 6. DTA curve of amorphous chromium hydroxide (sample C10) obtained in argon.

observed in sample C11, indicated a difference in the chemistry of thermal decomposition in oxidative (air, oxygen) or reductive (nitrogen, argon) atmospheres. It is realistic to suppose that the accelerated crystallization of Cr_2O_3 from amorphous chromium hydroxide in air involved a catalytic effect of higher oxidation states of chromium. Chromium species were probably restricted to the surface of the particles. However, if they were also present in the bulk, their conversion to the initial Cr(III) state was complete, so that they could not be observed by XRD. Schroeder et al.[35] monitored in situ thermal dehydration of hydrous chromium hydroxide gel using total electron-yield XAS (X-ray absorption spectroscopy). The authors found that amorphous chromium hydroxide was partially oxidized in argon atmosphere (Cr(III)→Cr(VI) and possibly Cr(V)). Taking into account the results obtained in the present work, it can be concluded that the chromium oxidation process in an argon atmosphere, as observed by Schroeder et al.,[35] was not able to catalyze the crystallization of Cr_2O_3 at lower temperatures, as it was observed in the experiments performed in air atmosphere. For this reason, the sharp exothermic peak of the Cr_2O_3 crystallization shifted to a significantly higher temperature (600 °C).
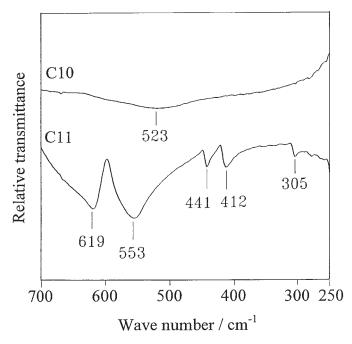
Figure 7. FT-IR spectra of amorphous chromium hydroxide (sample C10) and its thermal decomposition product obtained at 650 °C in argon (sample C11). The spectra were recorded at room temperature.

CONCLUSION

The conditions of the forced hydrolysis of a solution of $Cr(NO_3)_3$ and urea were investigated. In decomposing urea a significant pH-increase could be achieved, thus accelerating the hydrolysis of Cr^{3+} ions. Phase analysis of hydroxide precipitates showed their amorphous character for the final pH values up to ~9 to 9.5 and for long times of aging, up to 60 days.

Heating amorphous chromium hydroxide samples at lower temperature, up to 360 °C, produced Cr_2O_3 crystallites of the order of 20 nm. However, after heating up to 825 °C, the crystallite size of Cr_2O_3 increased to the order of 100 nm. Crystallization from amorphous chromium hydroxide was also monitored by FT-IR spectroscopy. The FT-IR spectra obtained in the present work were compared with the spectrum of commercial Cr_2O_3 (purity 99.999%).

TGA/DTA curves recorded in air showed thermal behavior of the samples that differed depending on the hydrolysis conditions, *i.e.* the initial concentration of urea. The endothermic peak due to water loss varied between 200 and 235 °C and was intersected by two exothermic peaks at 265 to

290 °C and 325 to 340 °C, respectively. A sharp exothermic peak between 410 and 420 °C, due to the crystallization of Cr_2O_3, was observed.

FT-IR spectrum of Cr_2O_3, produced in argon atmosphere, showed a pronounced IR band at 619 cm^{-1}, a strong suppression of the band at 656 cm^{-1} and a strong decrease of the relative intensity of the band at 412 cm^{-1}. For the same sample, an exothermic shift to 600 °C in the DTA curve was observed. It was suggested that the accelerated crystallization of Cr_2O_3 from amorphous chromium hydroxide in air involved a catalytic effect of higher oxidation states of chromium species, probably restricted at the surface of particles. In the next step, chromium species of higher oxidation states converted to the initial Cr(III) state. The catalytic effect of higher oxidation states of chromium was not involved during the Cr_2O_3 crystallization from amorphous chromium hydroxide in argon atmosphere, or it was very small, and, for this reason, the sharp exothermic peak of the Cr_2O_3 crystallization shifted to 600 °C.

REFERENCES

1. R. Demchak and E. Matijević, *J. Coll. Interface Sci.* **31** (1969) 257–262.
2. A. Bell and E. Matijević, *J. Phys. Chem.* **78** (1974) 2621–2625.
3. A. Bell and E. Matijević, *J. Inorg. Nucl. Chem.* **37** (1975) 907–912.
4. R. Sprycha, J. Jablonski, and E. Matijević, *Colloids Surf.* **67** (1992) 101–107.
5. C. E. Giacomelli, M. J. Avena, O. R. Camara, and C. P. De Pauli, *J. Coll. Interface Sci.* **169** (1995) 149–160.
6. M. Siddiq, T. Gilanyi, and A. C. Zettlemoyer, *J. Coll. Interface Sci.* **64** (1978) 192–193.
7. A. Kawabata, M.Yoshinaka, K. Hirota, and O. Yamaguchi, *J. Am. Ceram. Soc.* **78** (1995) 2271–2273.
8. B. Hou, X. Ji, Y. Xie, J. Li, B. Shen, and Y. Qian, *NanoStructured Mater.* **5** (1995) 599–605.
9. T. Maruyama and H. Akagi, *J. Electrochem. Soc.* **143** (1996) 1955–1958.
10. M. Maciejewski, K. Köhler, H. Schneider, and A. Baiker, *J. Solid State Chem.* **119** (1995) 13–23.
11. N. E. Fouad, H. Knözinger, M. I. Zaki, and S. A. A. Mansour, *Z. Phys. Chem.* **171** (1991) 75–96.
12. M. A. Vuurman, I. E. Wachs, D. J. Stufkens, and A. Oskam, *J. Molec. Catal.* **8** (1993) 209–227.
13. B. M. Weckhuysen, L. M. Ridder, and R. A. Schoonheydt, *J. Phys. Chem.* **97** (1993) 4756–4763.
14. B. M. Weckhuysen and I. E. Wachs, *J. Chem. Soc., Faraday Trans.* **92** (1996) 1969–1973.
15. Th. Schedel – Niedrig, Th. Neisius, C. T. Simmons, and K. Köhler, *Langmuir* **12** (1996) 6377–6381.
16. J. Engweiler, J. Nickl, A. Baiker, K. Köhler, C. W. Schläpfer, and A. Von Zelewsky, *J. Catal.* **145** (1994) 141–150.

17. U. Scharf, H. Schneider, A. Baiker, and A. Wokaun, *J. Catal.* **145** (1994) 464–478.
18. H. Schneider, U. Scharf, A. Wokaun, and A. Baiker, *J. Catal.* **146** (1994) 545–556.
19. K. Köhler, M. Maciejewski, H. Schneider, and A. Baiker, *J. Catal.* **157** (1995) 301–311.
20. H. Schneider, M. Maciejewski, K. Köhler, A. Wokaun, and A. Baiker, *J. Catal.* **157** (1995) 312–320.
21. S. Musić, S. Popović, and M. Ristić, *J. Mater. Sci.* **28** (1993) 632–638.
22. S. Musić, M. Lenglet, S. Popović, B. Hannoyer, I. Czakó-Nagy, M. Ristić, D. Balzar, and F. Gashi, *J. Mater. Sci.* **31** (1996) 4067–4076.
23. A. Rousset and J. Pâris, *Bull. Soc. Chim. France* (1967) 3888–3895.
24. D. R. Rennneke and D. W. Lynch, *Phys. Rev.* **138** (1965) A530-A533.
25. C. J. Serna, J. L. Rendon, and J. E. Iglesias, *Spectrochim. Acta* **38A** (1982) 797–802.
26. M. Lenglet, R. Guillamet, J. Lopitaux, and B. Hannoyer, *Mat. Res. Bull.* **25** (1990) 715–722.
27. D. Scarano and A. Zecchina, *Spectrochim. Acta* **43A** (1987) 1441–1445.
28. K. Hadjiivanov and G. Busca, *Langmuir* **10** (1994) 4534–4541.
29. K. I. Hadjiivanov, D. G. Klissurski, and V. Ph. Bushev, *J. Chem. Soc., Faraday Trans.* **91** (1995) 149–153.
30. J. D. Carruthers, K. S. W. Sing, and J. Fenetry, *Nature, London*, **213** (1967) 66–68.
31. J. D. Carruthers and K. S. W. Sing, *Chem. Ind.* No.11, (1967) 1919–1920.
32. P. Ratnasamy and A. J. Léonard, *J. Phys. Chem.* **76** (1972) 1838–1843.
33. D. G. Klissurski and V. N. Bluskov, *Can. J. Chem.* **61** (1983) 457–460.
34. R. Giovanoli and W. Stadelmann, *Thermochim. Acta* **7** (1973) 41–55.
35. S. L. M. Schroeder, G. D. Moggridge, T. Rayment, R. M. Lambert, *J. Phys. IV France* **7** (1997) C2 923-C2 924.

SAŽETAK

Nastajanje krom(III) oksida iz amorfnog krom(III) hidroksida

Svetozar Musić, Miroslava Maljković, Stanko Popović i Rudolf Trojko

Istraživana je ubrzana hidroliza iona Cr^{3+} u otopini $Cr(NO_3)_3$ i uree pri 100 i 90 °C. Talozi kromova(III) hidroksida bili su amorfni do pH ≈ 9–9.5 i vremena starenja do 60 dana pri 90 °C. Grijanjem amorfnog kromova(III) hidroksida do 360 °C dobiveni su kristali Cr_2O_3 veličine ≈ 20 nm, dok su grijanjem ishodnog materijala do 825 °C dobiveni kristali Cr_2O_3 veličine ≈ 100 nm. Kristalizacija Cr_2O_3 također je motrena primjenom FT-IR spektroskopije. Krivulje TGA/DTA, snimljene u zraku, pokazale su različito termičko ponašanje amorfnog kromova(III) hidroksida u ovisnosti o eksperimentalnim uvjetima. Oštar egzotermni vrh između 410 i 420 °C dobiven je zbog kristalizacije Cr_2O_3. Taj egzotermni vrh pomaknuo se na 600 °C kada je amorfni kromov(III) hidroksid zagrijavan u argonu. Ubrzana kristalizacija Cr_2O_3 iz amorfnog kromova(III) hidroksida u zraku objašnjena je katalitičkim efektom spojeva kroma s višim oksidacijskim brojevima. Ti spojevi kroma, vjerojatno ograničeni na površinu čestica, nisu bili stabilni i reducirali su se u početni Cr^{3+}. Rentgenske difrakcijske slike praha pokazale su samo nastajanje faze Cr_2O_3.